OPEN ACCESS Freely available online

PLoS one

Probing High Affinity Sequences of DNA Aptamer against $VEGF_{165}$

Harleen Kaur, Lin-Yue Lanry Yung*

Department of Chemical and Biomolecular Engineering, National University of Singapore, Singapore, Singapore

Abstract

Vascular endothelial growth factor ($VEGF_{165}$) is a potent angiogenic mitogen commonly overexpressed in cancerous cells. It contains two main binding domains, the receptor-binding domain (RBD) and the heparin-binding domain (HBD). This study attempted to identify the specific sequences of the VEa5 DNA aptamer that exhibit high binding affinity towards the $VEGF_{165}$ protein by truncating the original VEa5 aptamer into different segments. Using surface plasmon resonance (SPR) spectroscopy for binding affinity analysis, one of the truncated aptamers showed a >200-fold increase in the binding affinity for HBD. This truncated aptamer also exhibited high specificity to HBD with negligible binding affinity for $VEGF_{121}$, an isoform of VEGF lacking HBD. Exposing colorectal cancer cells to the truncated aptamer sequence further confirmed the binding affinity and specificity of the aptamer to the target $VEGF_{165}$ protein. Hence, our approach of aptamer truncation can potentially be useful in identifying high affinity aptamer sequences for the biological molecules and targeting them as antagonist for cancer cell detection.

Citation: Kaur H, Yung L-YL (2012) Probing High Affinity Sequences of DNA Aptamer against $VEGF_{165}$. PLoS ONE 7(2): e31196. doi:10.1371/journal.pone.0031196

Editor: Christina Lynn Addison, Ottawa Hospital Research Institute, Canada

Received September 21, 2011; **Accepted** January 3, 2012; **Published** February 16, 2012

Funding: This work was supported by research funding from the Singapore Ministry of Education Academic Research Fund Tier 2 grant MOE2008-T2-1-046 and Tier 1 grant R279000282112. The funders had no role in study design, data collection and analysis, decision to publish, or preparation of the manuscript.

Competing Interests: The authors have declared that no competing interests exist.

* E-mail: cheyly@nus.edu.sg

Introduction

Short single stranded nucleic acids referred to as aptamers are widely being explored as molecules of high affinity and specificity for binding a diverse array of target molecules ranging from high molecular weight proteins to small ions and nucleotides [1–3]. Aptamers contain functional moieties that fold into different secondary conformations, such as hairpin stem and loops, G-quadruplexes, bulges and pseudoknots, and they exhibit substantial impact on the conformational stability and target binding affinity of the aptamer. The non-immunogenic property of aptamer provides additional advantage over the prevalent antibodies and makes them a promising candidate for therapeutic and diagnostic application [4]. ''Macugen'' is the first FDA-approved aptamer-based therapeutic for treating the wet-form of age-related macular degeneration. The successful approval of this 27-mer RNA aptamer as therapeutic drug in 2004 has demonstrated the potential of aptamers as future therapeutics [5]. Currently, 8 aptamers are in various phases of clinical trials for treating different diseases [6–13]. These include NOX-E36 L-RNA aptamer against CCL2 ligand in Type 2 diabetes, G-quadruplex forming AS1411 DNA aptamer against nucleolin in acute myeloid leukemia, and phosphorothioate-modified ARC1779 DNA aptamer against von Willebrand factor (vWF) in carotid artery disease [7,8,10].

Aptamers are commonly screened and obtained by *in vitro* selection technique, also termed as systematic evolution of ligands by exponential enrichment (SELEX). SELEX starts with a random pool of oligonucleotide library incubated with the target molecule and involves continuous rounds of affinity and amplification steps to screen for the high affinity sequences [14,15]. Different selection process has been used for isolation of high binding affinity aptamers in SELEX, such as nitrocellulose membrane filtration, surface plasmon resonance (SPR), capillary electrophoresis and bead-based methods [15–18]. Binding affinity and specificity are the crucial criteria for the therapeutic use of aptamers. Generally, not all nucleotide domains of the post-screened aptamer play an important role in target binding. The non-binding domain may actually interfere with the interaction between the aptamer and target protein by formation of complex secondary structures, and eventually prevents the binding domain to fold into the desired conformation for binding to the target [4]. This may result in reduction or complete loss of the binding affinity as well as higher synthesis cost. Therefore, identifying the high binding affinity domains in the post-screened aptamer is a key step to perform for producing potent aptamers with higher affinity/specificity for various biomedical applications.

Different strategies have been adopted to enhance the aptamer binding affinity for its target and to make them suitable for different biological applications. One of the commonly used strategies includes chemical modification of the aptamer structure at 5′- or 3′-terminus, nucleobase, sugar, and phosphate backbone. The modifications include (i) the addition of functional groups, such as amino (-NH_2), fluoro (-F), *O*-methyl (-OCH_3), locked nucleic acids (LNAs) or phosphorothioate linkages (PS-linkages) to make aptamers nuclease resistant, and (ii) conjugation with high molecular weight polyethylene glycol (PEG) to enhance *in vivo* circulating half-life [5,19–26]. Apart from improving the stability of the aptamer, these modifications can improve the affinity of the aptamer in the cellular environment. Additionally, software algorithms have been used to deduce the binding domains by comparing different sequences as well as to predict the secondary

structure [27,28]. Strategies such as partial fragmentation, enzymatic footprinting, and recently microarray based binding sequence determination have also been employed for probing the high affinity binding sequences [13,29,30].

Vascular endothelial growth factor (VEGF) is a mitogenic protein secreted by both endothelial and tumor cells and induces physiological and pathological angiogenesis inside the body. Through alternate exon splicing of single human VEGF gene, several isoforms of this growth factor, including $VEGF_{165}$, $VEGF_{121}$, $VEGF_{189}$ and $VEGF_{206}$, are generated [31]. Of these, $VEGF_{165}$ and $VEGF_{121}$ are the predominant isoforms. $VEGF_{165}$, which contains both heparin-binding domain (HBD) and receptor-binding domain (RBD), has been shown to be a more potent mitogen in inducing angiogenesis compared with $VEGF_{121}$, which contains only RBD [32–34].

A previous work by Ikebukuro and co-workers has identified a 66mer DNA aptamer (VEa5) that binds to HBD of $VEGF_{165}$ protein with K_d value of 130 nM [35]. Since increasing the binding affinity of this aptamer is important for further therapeutic development, they later adopted the dimerization method to reduce the K_d of VEa5 aptamer to 6 nM, which is 20 times better than the original monomeric VEa5 [36]. In the present study, we adopted a different strategy to improve the binding affinity of the VEa5 aptamer. We attempted to identify the high affinity binding sequences within the 66mer VEa5 by truncating its stem-loop regions and investigated the impact on the binding affinity against HBD of $VEGF_{165}$ protein using surface plasmon resonance (SPR) spectroscopy. Our results demonstrated that the truncation of the stem-loop regions can locate the key binding domain in the aptamer and the truncated sequence exhibits substantially higher binding affinity compared with the entire VEa5 aptamer. *In vitro* binding study with colorectal cancer cells overexpressed with VEGF protein further confirmed the high binding affinity of the truncated aptamer.

Materials and Methods

Materials

The HPLC purified oligonucleotides (both unlabeled and fluorescent-labeled) were purchased from Sigma-Aldrich. The recombinant human carrier free $VEGF_{165}$ (molecular weight of 38 kDa, pI = 8.25) and $VEGF_{121}$ (molecular weight of 28 kDa, pI = 6.4) proteins were purchased from R & D systems. CM5 sensor chips were purchased from GE Healthcare for protein immobilization. 1-ethyl-3-[3-dimethylaminopropyl] carbodiimide hydrochloride (EDC), N-hydroxysuccinimide (NHS), and ethanol-amine-HCl were purchased from Sigma-Aldrich. Sodium acetate (anhydrous) was purchased from Fluka. Human colorectal adenocarcinoma HT-29 cell line was a gift from Dr. Partha Roy's lab. Normal human fetal lung fibroblast MRC-5 cells were obtained from ATCC. Dulbecco's modified eagle's media (DMEM) media, RPMI-1640 and fetal bovine serum (FBS) was purchased from Caisson laboratories. Trypsin-EDTA and 1% penicillin/streptomycin mixture were purchased from PAN biotech. Phosphate buffer saline (PBS) buffer was purchased from 1st Base. Tween-20 was purchased from USB Corporation.

Binding affinity of truncated aptamers via surface plasmon resonance spectroscopy

To elucidate the role of stem-loop regions of the VEa5 aptamer in VEGF binding, the original sequence of the VEa5 was truncated. The corresponding binding affinity of truncated aptamers was investigated using surface plasmon resonance (SPR) spectroscopy, where $VEGF_{165}$ and $VEGF_{121}$ acted as ligands and were directly immobilized on the sensor chip. Briefly, the carboxylic group on the sensor chip was activated by standard amine coupling procedure using freshly prepared EDC/NHS. $VEGF_{165}$ or $VEGF_{121}$ (25 μg/ml) in acetate buffer (pH 6.0) was then injected into the sensor chip at flow rate 8 μl/min to reach ~200RU immobilization level. The deactivation was done by ethanolamine-HCl to block unreacted carboxyl groups. The binding analysis was carried out with truncated aptamers at different concentrations (0.2 to 100 nM) using a BIAcore 2000 instrument (GE Healthcare). The running condition was set at 30 μl/min flow rate, 25°C, 3 min association time and 5 min dissociation time. PBS and 0.005% tween-20 solution mixture was used as the running buffer, and 50 mM NaOH as the regeneration buffer. All the buffers were filtered and degassed prior to each experiment. Blank surfaces were used for background subtraction. Upon injection of the truncated aptamers, sensorgrams recording the association/dissociation behavior of the VEGF-aptamer complex were collected. By varying the truncated aptamer concentration, a series of sensorgrams (Figure 1) were obtained and subsequently analyzed using the 1:1 Langmuir model provided in the BIAevaluation software (version 4.1) to calculate the equilibrium dissociation constant K_d. All SPR measurements were performed in triplicates.

Cellular binding of truncated aptamer via flow cytometry analysis

The HT-29 colorectal cancer and MRC-5 human fetal lung fibroblast cells were plated at a seeding density of 10^5 cells/ml in DMEM and RPMI-1640 media and were allowed to attach for 48 hours in humidified incubator containing 5% CO_2, 1% O_2 and 94% N_2 (hypoxia) at 37°C. The hypoxia condition was maintained by culturing the cells in a sealed hypoxia chamber (Billups-Rothenberg). The cells were trypsinized for very short time and incubated with 5′-PE-texas red labeled truncated aptamer of different concentrations for 2 hours at 37°C in culture medium. The cells were then centrifuged for 5 min at 1500 rpm and re-suspended in PBS buffer for flow cytometry analysis immediately. Analysis was performed on a Beckman-Coulter CyAn ADP flow cytometer using 488 nm excitation and 613/20 nm emission filter. 20,000 events were collected for each sample. All the experiments for binding assay were repeated at least 3 times. Relative fluorescence was determined using SUMMIT V 4.3.02 software. For calculation of equilibrium dissociation (K_d), the fluorescence intensity signal was plotted against fluorescently labeled aptamer concentration by fitting in equation $Y = B_{max}\ X/(K_d+X)$ using SigmaPlot software. Sequence specificity of the SL_2-B aptamer was determined using a scrambled sequence. The K_d value of the SL_2-B aptamer was calculated by subtracting the fluorescence intensity signal from the scrambled sequence.

Competitive aptamer binding assay was performed to determine the effect of unlabeled SL_2-B aptamer on the binding capability of 5′-PE-texas red labeled truncated aptamer. HT-29 colorectal cancer cells were incubated with 20-fold excess concentration of unlabeled aptamer as competitor (10 nM) simultaneously with 5′-PE-texas red labeled aptamer (0.5 nM). All other experimental conditions and procedures were same as described for the flow cytometry analysis.

Fluorescence microscopy imaging

The HT-29 cells and MRC-5 cells were seeded in 24-well plate in DMEM and RPMI-1640 media respectively. Cells were plated at a seeding density of 10^5cells/ml in their individual media supplemented with FBS and penicillin/streptomycin mixture in the same hypoxic conditions as mentioned above. Subsequently,

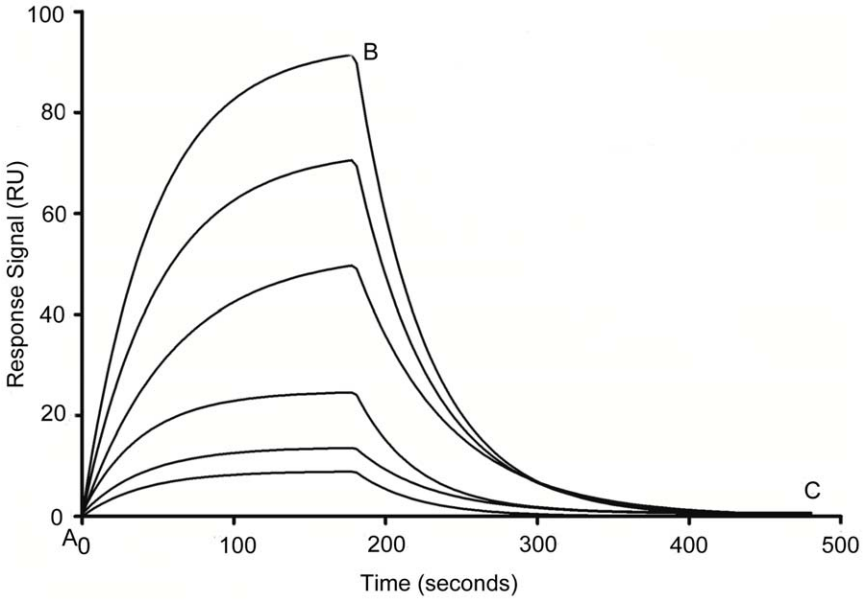

Figure 1. Typical SPR sensorgrams demonstrating interaction of aptamer with immobilized $VEGF_{165}$ protein at different concentrations (bottom to top, 0.2 to 100 nM). Point A to B corresponds to the association phase and point B to C corresponds to the dissociation phase in all the sensorgrams. Shown here is the SL_2-B aptamer ($K_d = 0.50 \pm 0.32$ nM).
doi:10.1371/journal.pone.0031196.g001

the cells were incubated with 5′-PE-texas red labeled truncated aptamer at 37°C for 2 hours and washed with PBS (pH = 7.4) three times to remove unbound aptamer. Sequence specificity of the truncated aptamer was determined using a scrambled sequence as control. Images of aptamer binding to cells were acquired using a Leica DMIL fluorescence microscope.

Statistical analysis

Results from at least 3 independent experiments in flow cytometry experiment were analyzed using Student's t-test. p-value$<$0.05 was considered significant. Data are expressed as mean ± S.D.

Results and Discussion

Binding analysis of aptamer-VEGF complex by surface plasmon resonance (SPR)

The induction of the aptamer folding was done using predictions by the mfold software [37]. As shown in Figure 2, VEa5 displays complex hairpin stem-loop secondary structure with three stem-loop regions and several unpaired terminal nucleotides. Based on the SPR measurement, the original VEa5 aptamer exhibited a binding constant of $K_d = 120$ nM to the surface immobilized $VEGF_{165}$ (Table 1). This value is very close to the K_d value of the VEa5 aptamer binding to the heparin-binding domain (HBD) of $VEGF_{165}$ reported in the literature ($K_d = 130$ nM) [35].

To better understand the significance of stem-loop (SL) regions towards binding affinity, we conducted a few truncations on the SL regions. By truncating SL_3 at the 3′ end together with 3′-termini hanging nucleotides and the nucleotides between SL_2 and SL_3, we obtained SL_{12} (Figure 3A and Table 1) and it exhibited a K_d value of 5 nM, a striking 24-fold increase in the binding affinity compared with the original VEa5 aptamer. Further truncation of SL_2 to yield SL_1 (Figure 3B and Table 1), however, resulted in complete loss of binding activity towards $VEGF_{165}$. These two modifications pointed to the indispensable role of SL_2 in the binding process. The increase in the binding affinity could be due to the deletion of non-binding nucleotides that hampers the

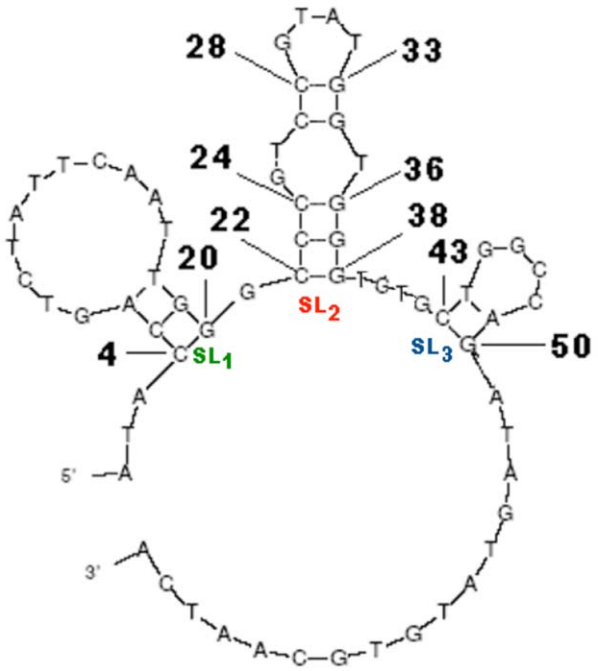

Figure 2. Schematic representation of the secondary structure of original VEa5 aptamer as predicted by the mfold program. Nucleotide 4–20 forms the stem-loop 1 (SL_1) region, nucleotide 22–38 forms the stem-loop 2 (SL_2) region, and nucleotide 43–50 forms stem-loop 3 (SL_3) region. Nucleotide 28–33 forms internal loop 1 (IL_1), and nucleotide 24–27+34–36 together forms internal loop 2 (IL_2) within SL_2 region.
doi:10.1371/journal.pone.0031196.g002

Table 1. Different aptamer sequences along with their equilibrium dissociation constant (K_d) values determined using surface plasmon resonance (SPR) spectroscopy.

Sequences of original and various truncated aptamers (5′------ 3′)*	K_d
VEa5 ATACCAGTCTATTCAATTGGGCCCGTCCGTATGGTGGGTGTGCTGGCCAGATAGTATGTGCAATCA	120±1.8 nM
SL_{12} ATACCAGTCTATTCAATTGGGCCCGTCCGTATGGTGGGTGTGCTGGCCAGATAGTATGTGCAATCA	5±0.45 nM
SL_1 ATACCAGTCTATTCAATTGGGCCCGTCCGTATGGTGGGTGTGCTGGCCAGATAGTATGTGCAATCA	No Binding
SL_2 ATACCAGTCTATTCAATTGGGCCCGTCCGTATGGTGGGTGTGCTGGCCAGATAGTATGTGCAATCA	49±2.4 nM
SL_2-A ATACCAGTCTATTCAATTGGGCCCGTCCGTATGGTGGGTGTGCTGGCCAGATAGTATGTGCAATCA	10±1.1 nM
SL_2-B ATACCAGTCTATTCAATTGGGCCCGTCCGTATGGTGGGTGTGCTGGCCAGATAGTATGTGCAATCA	0.5±0.32 nM

*The underlined and bold section indicates the aptamer sequence and the non-bold grey section indicates the truncated sequence. In aptamer sequence terminology, the subscript number indicates the presence of the particular stem-loop region.

doi:10.1371/journal.pone.0031196.t001

binding process and hence, their removal may lead to more desired secondary conformation in the truncated aptamer required for binding to the HBD of $VEGF_{165}$ protein [28].

We next truncated SL_1 and left with only the SL_2 sequence for $VEGF_{165}$ binding analysis, and surprisingly we obtained lower binding affinity. With K_d value of 49 nM (Figure 3C and Table 1), the binding affinity of the SL_2 sequence was approximately 10 times higher than the K_d of SL_{12}. This prompted us to further investigate the role of the additional sequence next to the 3′ and 5′ ends of the SL_2 region. By adding a single nucleotide at both 5′ and 3′-ends of the SL_2 aptamer (SL_2-A, Figure 3D), we were able to lower the K_d value by almost 5-fold ($K_d = 10$ nM, Table 1) compared to the SL_2 aptamer. Further addition of nucleotides to 3′-end did not yield any improvement in the binding affinity. However, adding another 7 nucleotides at 5′-end of the SL_2 aptamer (SL_2-B, Figure 3E) showed further enhancement in the binding affinity ($K_d = 0.5$ nM, Table 1), and this represented a 90-fold increase compared with the SL_2 aptamer, and more than 200-fold increase compared with the original VEa5 aptamer and 10-fold increase compared with the dimerized VEa5 aptamer [36]. A possible explanation is that the addition of nucleotides to the 5′-end provides more conformational stability to the aptamer which

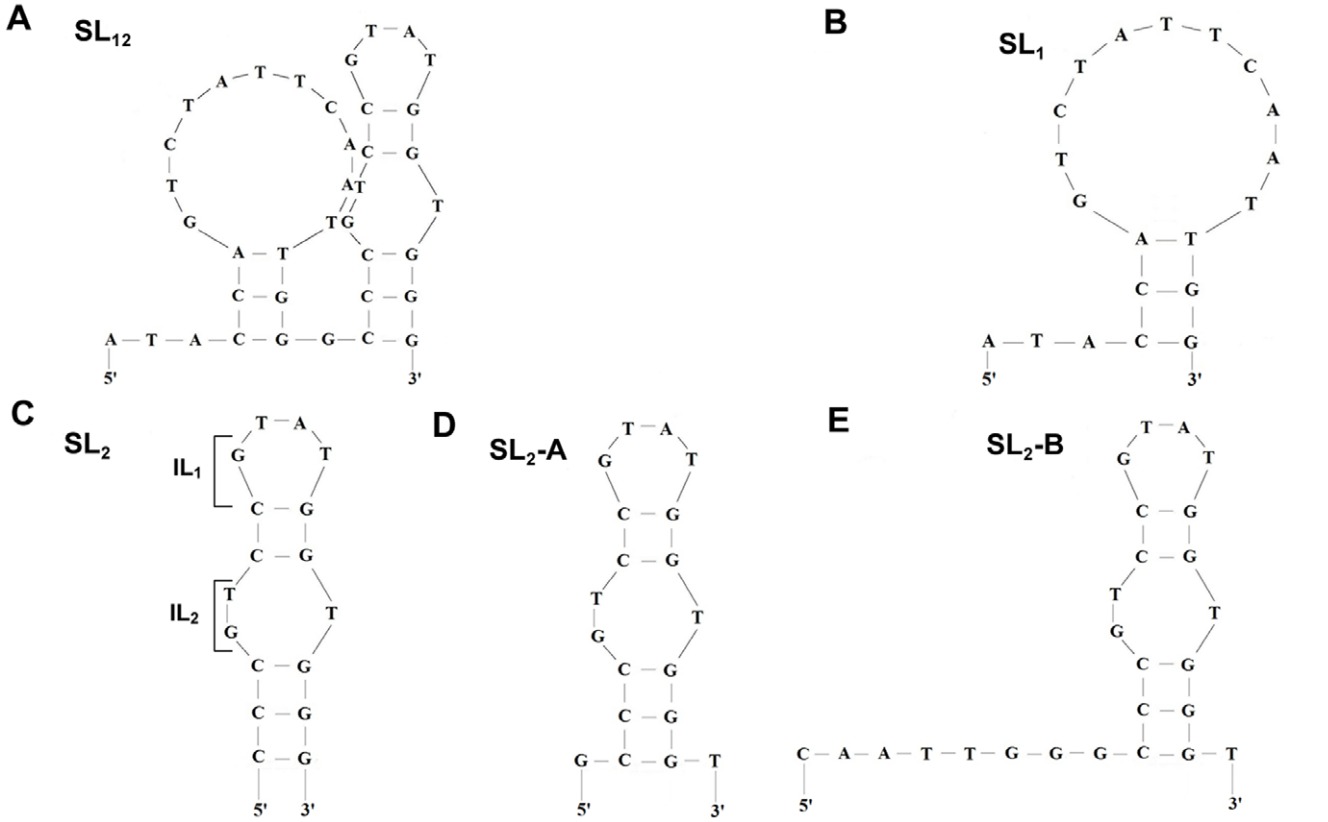

Figure 3. Schematic representation of the secondary structures of various truncated aptamers as predicted by the mfold program. (A) SL_{12} indicates the presence of SL_1 and SL_2 regions together, (B) SL_1 indicates the presence of SL_1 region only and (C) SL_2 indicates the presence of SL_2 region only. (D) SL_2-A and (E) SL_2-B correspond to secondary structures formed after addition of nucleotides to SL_2 region.

doi:10.1371/journal.pone.0031196.g003

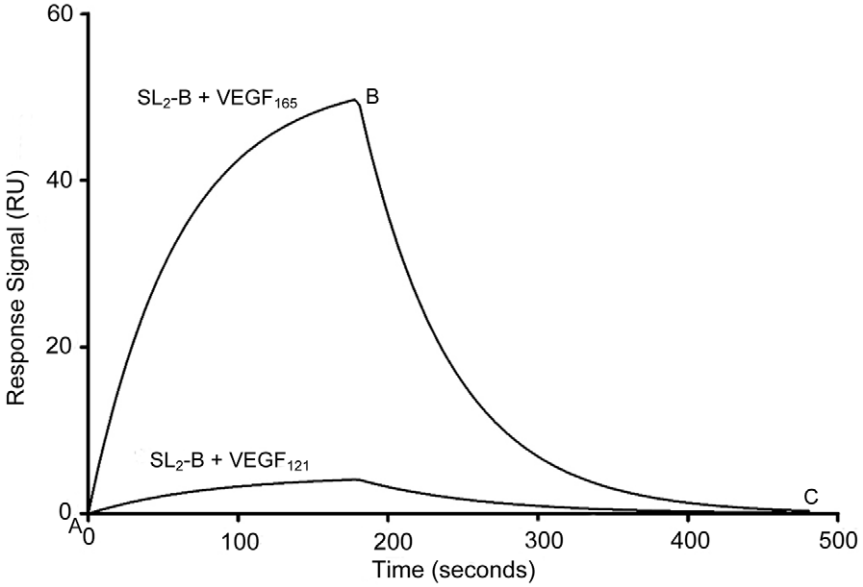

Figure 4. Sensorgrams demonstrating interaction of SL_2-B aptamer with immobilized $VEGF_{165}$ and $VEGF_{121}$ proteins using SPR spectroscopy. Point A to B corresponds to the association phase and point B to C corresponds to the dissociation phase in the sensorgrams. Shown here is SL_2-B aptamer binding with $VEGF_{165}$ protein ($K_d = 0.50 \pm 0.32$ nM) and $VEGF_{121}$ protein ($K_d = 10.2 \pm 1.89$ μM).
doi:10.1371/journal.pone.0031196.g004

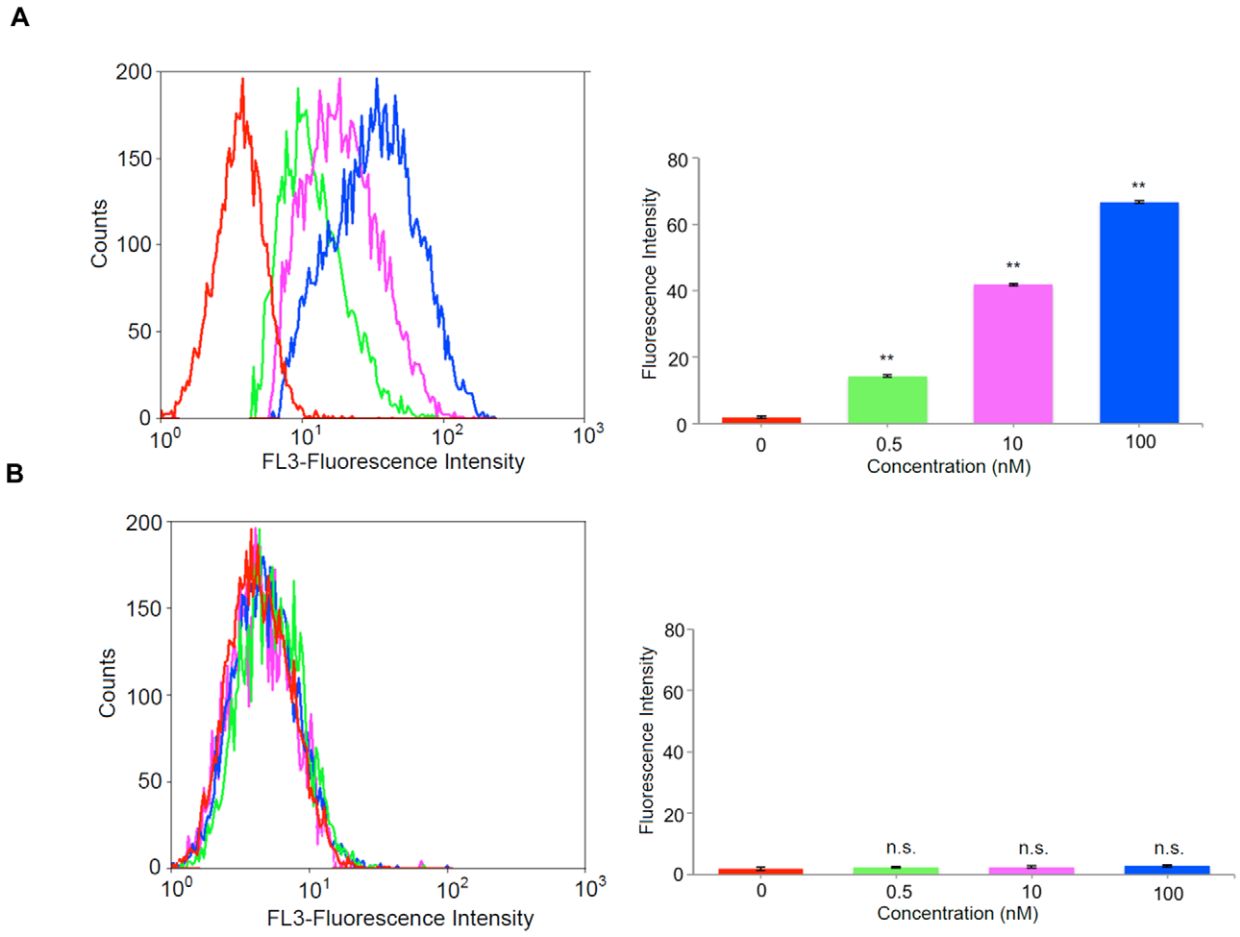

Figure 5. Representative flow cytometry profiles and quantitative analysis of flow cytometry results in (A) HT-29 cells and (B) MRC-5 cells after SL_2-B aptamer at different concentrations (red – 0 nM (negative control), green – 0.5 nM, pink – 10 nM, blue – 100 nM), **Significant difference compared with the negative control (p-value<0.001), n.s. – not significant.
doi:10.1371/journal.pone.0031196.g005

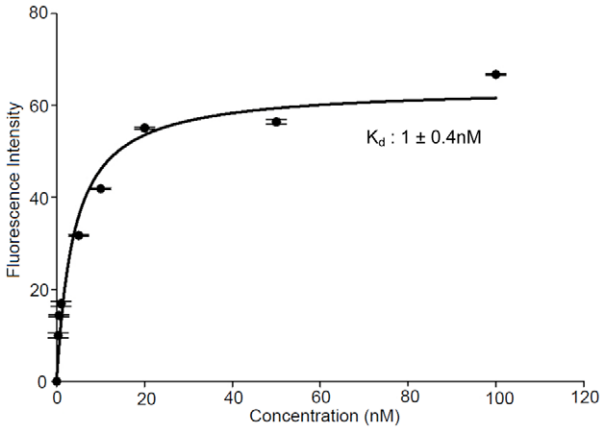

Figure 6. Binding curve of SL_2-B aptamer with HT-29 cells. Cells were incubated with different SL_2-B aptamer concentrations ranging from 0 to 100 nM. The fluorescence intensity originating from the scrambled sequence at each concentration was subtracted from the fluorescence intensity of corresponding SL_2-B aptamer. The actual fluorescence intensity was fitted into SigmaPlot software to determine the K_d.
doi:10.1371/journal.pone.0031196.g006

helps in improving the binding competence of the SL_2-B sequence [38]. We also attempted to truncate the internal loops of SL_2 (IL_1 and IL_2, Figure 2) but the removal of either loops reduced the binding affinity. Therefore, SL_2-B is thought to be the minimal sequence required in VEa5 aptamer to provide high binding affinity to HBD of $VEGF_{165}$.

To address the selectivity of the truncated SL_2-B aptamer to $VEGF_{165}$ binding, $VEGF_{121}$ was selected for the binding comparison. $VEGF_{121}$ is another spliced form of VEGF mRNA that constitutes only the receptor-binding domain (RBD) but is devoid of HBD. HBD assists in the binding of VEGF protein to the heparin sulfate (HS) and heparin sulfate proteoglycans (HSPGs) present on the extracellular matrix of the cell membrane [32]. This enhances the interaction of VEGF with its receptors (VEGFR-1/Flt-1 and VEGFR-2/KDR) and the specific co-receptor neuropilins, triggering the cellular angiogenic response in malignant cells [34].

Compared with $VEGF_{165}$, the binding of $VEGF_{121}$ to the membrane receptors is not strong, making it not potent to generate intense angiogenic signal. Using SL_2-B for binding analysis with $VEGF_{121}$ under same buffer condition (Figure 4), substantial reduction in the response signal and minimal binding (K_d = 10.2 μM) was observed compared to $VEGF_{165}$. This confirms the binding selectivity of the truncated SL_2-B aptamer on HBD of the $VEGF_{165}$ protein.

In vitro cellular binding analysis of SL_2-B aptamer-VEGF complex

Compared to techniques such as nitrocellulose membrane filtration or capillary electrophoresis, cell-based technique, such as flow cytometry, isolates aptamer sequences that have the ability to bind to their target with high affinity and specificity in a more physiologically relevant environment [39,40]. Thus, it has been considered as a more direct strategy for studying the binding of aptamers to their targets on cellular surface.

To validate the increase in the binding affinity of the truncated SL_2-B aptamer and to determine its target specificity at cellular level, we exposed the fluorescent-labeled SL_2-B sequence directly on the HT-29 colorectal cancer cells and normal MRC-5 fibroblast cells (control) under 1% O_2 hypoxia condition by flow cytometry analysis. As shown in Figure 5A, a significant peak shift (increase in the fluorescent signal) was observed for SL_2-B aptamer at different concentrations, compared to control sample (only cells) in response to hypoxia conditions in HT-29 cells (p-value$<$0.001). The percentage of fluorescent-labeled cells increased with the increase in the concentration of the SL_2-B aptamer, indicating the binding of the SL_2-B aptamer to the cell surface. In contrast, when using normal MRC-5 fibroblast cells, no enhancement in the fluorescent signal was observed after treatment with different SL_2-B aptamer concentrations (Figure 5B, not significant (n.s.) compared to negative control). Since the VEGF protein is overexpressed in HT-29 cells but not the normal MRC-5 cells, the result showed that SL_2-B can specifically form aptamer-VEGF complex on the HT-29 cell membrane. The K_d value of the SL_2-B towards VEGF was further evaluated using flow cytometry data (Figure 6). The K_d value for the SL_2-B aptamer to the cell surface was found to be 1.0 nM, which is close to the K_d value determined by SPR technique (Figure 6). Repeating the same experiment at

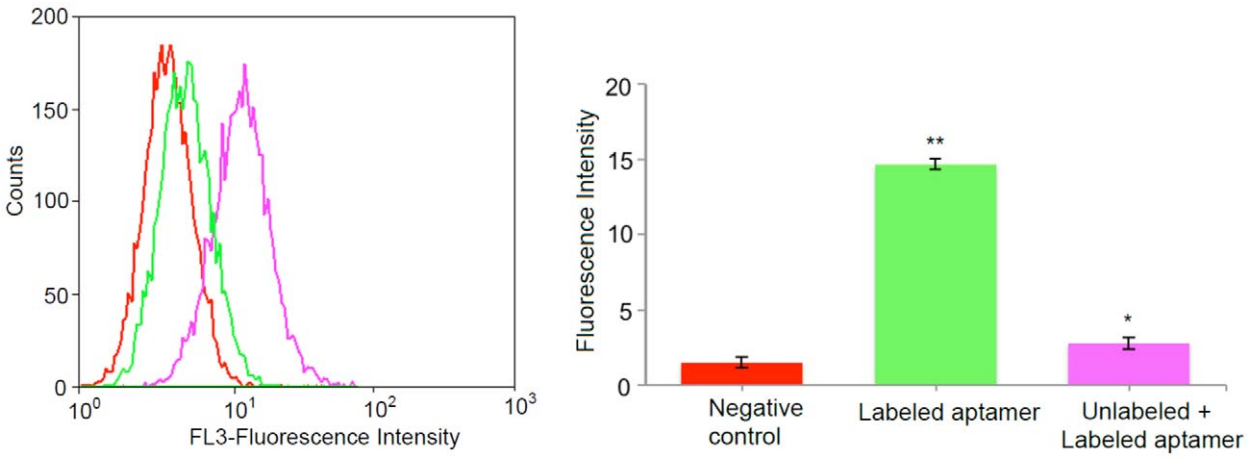

Figure 7. Flow cytometry histogram showing binding competition between the labeled and unlabeled SL_2-B aptamer in HT-29 cells and quantitative analysis of flow cytometry result. Red – 0 nM (negative control), green – aptamer binding without excess of unlabeled SL_2-B aptamer (0.5 nM); pink – aptamer binding in excess of unlabeled SL_2-B aptamer (unlabeled aptamer – 10 nM, labeled aptamer – 0.5 nM). *Significant difference from the negative control sample at p-value$<$0.05; **Significant difference from the negative control sample at p-value$<$0.001.
doi:10.1371/journal.pone.0031196.g007

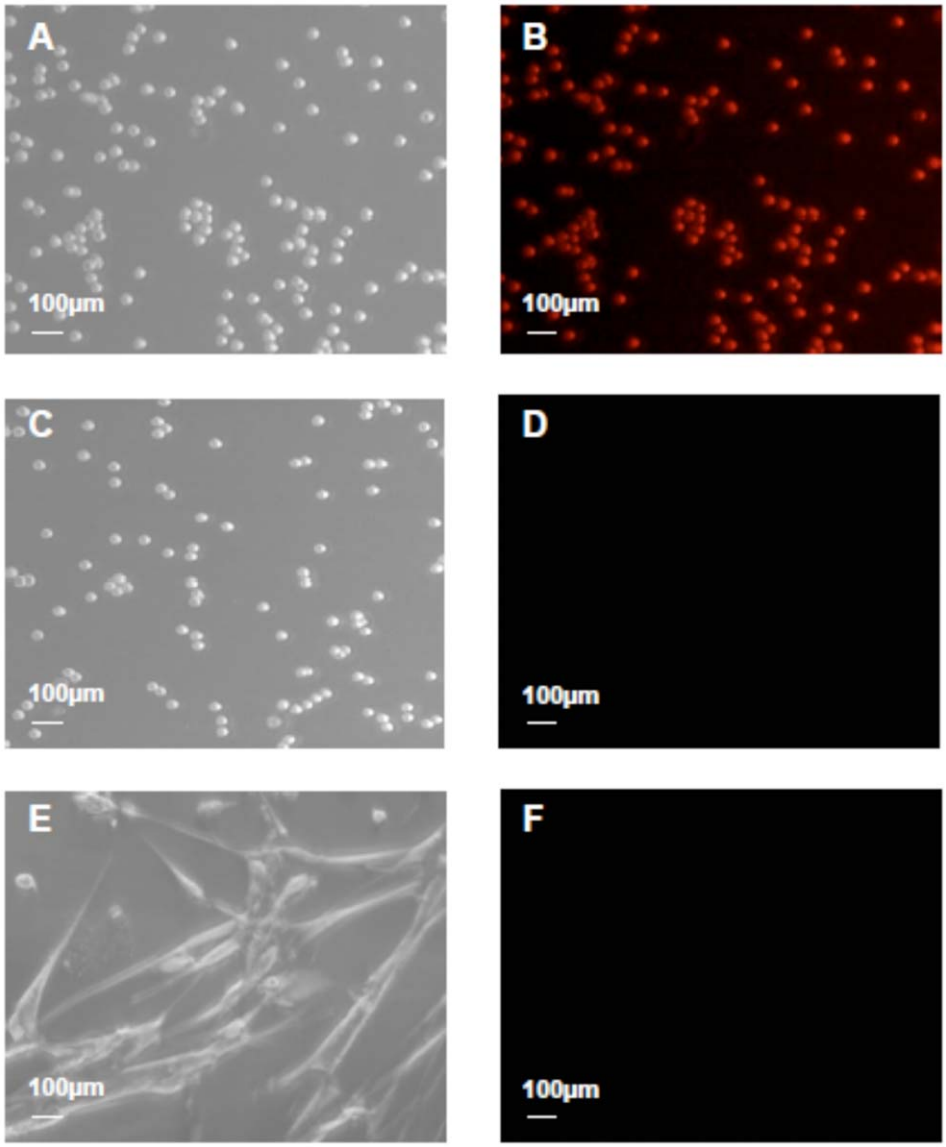

Figure 8. Binding of PE-texas red-labeled aptamers (SL_2-B and scrambled sequence) to HT-29 cells and normal MRC-5 fibroblast cells under hypoxia condition. (A) & (C) Bright field images of HT-29 cells after exposing to the SL_2-B and scrambled sequence respectively. (B) & (D) Corresponding fluorescence microscopy images of the (A) & (C) bright field images. (E) & (F) Bright field and fluorescence microscopy images of MRC-5 cells after exposing to the SL_2-B sequence.
doi:10.1371/journal.pone.0031196.g008

normoxia condition (i.e. 21% O_2) did not yield any observable binding of SL_2-B aptamer to the cells. The result is in agreement with the fact that the hypoxia condition enhances production of VEGF protein in HT-29 cells [41–43].

Hypoxia is one of the crucial physiological factors that exert profound impact on the metabolism, invasion and tumor progression, thereby affecting many oncogenic pathways. Inadequate level of cellular oxygen leads to aggressive phenotypic changes in the tumor cells, and is primarily responsible for their resistance against the therapies and poor prognosis [44]. Exposure to hypoxia milieu upregulates the expression of master regulator Hypoxia-Inducible Factor 1 gene (HIF-1 gene) in the solid tumors, which switch on the transcription of several downstream genes, in particular, VEGF [45]. The expression of VEGF protein and its two tyrosine kinase receptors – VEGFR-1/Flt-1 and VEGFR-2/KDR is induced by the transcription and stabilization of VEGF mRNA in response to hypoxia, resulting in increase rate of vascularization in tumor [46–48].

The binding ability of SL_2-B aptamer for VEGF protein in HT-29 cells was evaluated by competing 5′-PE-texas red labeled SL_2-B sequence against the unlabeled SL_2-B sequence. As shown in Figure 7, the presence of 20-fold excess of unlabeled aptamer significantly decreased the fluorescent signal from the PE-texas red labeled aptamer (p-value$<$0.05). This result suggests that both the labeled and unlabeled SL_2-B aptamer binds to the same target, the VEGF protein on HT-29 cell membrane.

In vitro fluorescence imaging of SL_2-B aptamer-VEGF complex

The targeting ability and specificity of the high affinity SL_2-B aptamer was further investigated and imaged using live colorectal cancer HT-29 cells and normal MRC-5 fibroblast cells (control) at

the same hypoxia conditions. By comparing the bright field and the fluorescent images, we observed red fluorescence on HT-29 cells after exposing to PE-texas red labeled SL_2-B aptamer (Figure 8A & B), but no detectable fluorescence was observed with PE-texas red labeled scrambled sequence (Figure 8C & D). This confirms the specific binding of SL_2-B aptamer to $VEGF_{165}$ protein in cancer cells. For MRC-5 fibroblasts, minimal fluorescence was also observed after exposing to the same SL_2-B aptamer (Figure 8E & F). This further demonstrates the specificity and targeting ability of the SL_2-B aptamer to cancer cells.

Conclusions

To summarize, this work attempted to identify in the key binding aptamer sequences by truncating based on the stem-loop structure of the original VEa5 aptamer. From the results, we can conclude that the SL_2 sequence is important for the binding to HBD of the $VEGF_{165}$ protein, and the SL_2-B aptamer binds HBD of $VEGF_{165}$ protein strongly and selectively. This newly obtained SL_2-B aptamer sequence can potentially be useful in oligomer-based cancer therapeutic and diagnostic applications, though further studies are required for better understanding of the SL_2-B aptamer sequence and to elucidate its binding mechanism with HBD of $VEGF_{165}$ protein. Furthermore, the current stem-loop modification approaches can be useful in identifying target domains, getting rid of excessive unnecessary nucleotides, and eventually lowering the cost of aptamer synthesis.

Acknowledgments

The authors thank Dr Partha Roy (Division of Bioengineering, National University of Singapore) for providing the HT-29 colorectal cancer cells. We also appreciated the doctoral scholarship (for H.K.) from NUS.

Author Contributions

Conceived and designed the experiments: HK LY. Performed the experiments: HK. Analyzed the data: HK LY. Contributed reagents/materials/analysis tools: HK LY. Wrote the paper: HK LY.

References

1. Bock LC, Griffin LC, Latham JA, Vermaas EH, Toole JJ (1992) Selection of single-stranded DNA molecules that bind and inhibit human thrombin. Nature 355: 564–566.
2. Wrzesinski J, Ciesiolka J (2005) Characterization of structure and metal ions specificity of Co^{2+}-binding RNA aptamers. Biochemistry 44: 6257–6268.
3. Davis JH, Szostak JW (2002) Isolation of high-affinity GTP aptamers from partially structured RNA libraries. Proc Natl Acad Sci USA 99: 11616–11621.
4. Jayasena SD (1999) Aptamers: An emerging class of molecules that rival antibodies in diagnostics. Clin Chem 45: 1628–1650.
5. Ruckman J, Green LS, Beeson J, Waugh S, Gillette WL, et al. (1998) 2′-fluoropyrimidine RNA-based aptamers to the 165-amino acid form of vascular endothelial growth factor (VEGF165): Inhibition of receptor binding and VEGF-induced vascular permeability through interactions requiring the exon 7-encoded domain. J Biol Chem 273: 20556–20567.
6. Sayyed SG, Hägele H, Kulkarni OP, Endlich K, Segerer S, et al. (2009) Podocytes produce homeostatic chemokine stromal cell-derived factor-1/CXCL12, which contributes to glomerulosclerosis, podocyte loss and albuminuria in a mouse model of type 2 diabetes. Diabetologia 52: 2445–2454.
7. Ninichuk V, Clauss S, Kulkarni O, Schmid H, Segerer S, et al. (2008) Late onset of Ccl2 blockade with the Spiegelmer mNOX-E36-3′-PEG prevents glomerulosclerosis and improves glomerular filtration rate in db/db mice. Am J Pathol 172: 628–637.
8. Bates PJ, Laber DA, Miller DM, Thomas SD, Trent JO (2009) Discovery and development of the G-rich oligonucleotide AS1411 as a novel treatment for cancer. Exp Mol Pathol 86: 151–164.
9. Waters EK, Richardson J, Schaub RG, Kurz JC (2009) Effect of NU172 and bivalirudin on ecarin clotting time in human plasma and whole blood. J Thromb Haemost 7: 683.
10. Diener JL, Daniel Lagassé HA, Duerschmied D, Merhi Y, Tanguay JF, et al. (2009) Inhibition of von Willebrand factor-mediated platelet activation and thrombosis by the anti-von Willebrand factor A1-domain aptamer ARC1779. J Thromb Haemost 7: 1155–1162.
11. Chan MY, Cohen MG, Dyke CK, Myles SK, Aberle LG, et al. (2008) Phase 1b randomized study of antidote-controlled modulation of factor IXa activity in patients with stable coronary artery disease. Circulation 117: 2865–2874.
12. Biesecker G, Dihel L, Enney K, Bendele RA (1999) Derivation of RNA aptamer inhibitors of human complement C5. Immunopharmacology 42: 219–230.
13. Green LS, Jellinek D, Jenison R, Ostman A, Heldin CH, et al. (1996) Inhibitory DNA ligands to platelet-derived growth factor B-chain. Biochemistry 35: 14413–14424.
14. Ellington AD, Szostak JW (1990) In vitro selection of RNA molecules that bind specific ligands. Nature 346: 818–822.
15. Tuerk C, Gold L (1990) Systematic evolution of ligands by exponential enrichment: RNA ligands to bacteriophage T4 DNA polymerase. Science 249: 505–510.
16. Misono TS, Kumar PKR (2005) Selection of RNA aptamers against human influenza virus hemagglutinin using surface plasmon resonance. Anal Biochem 342: 312–317.
17. Berezovski M, Drabovich A, Krylova SM, Musheev M, Okhonin V, et al. (2005) Nonequilibrium capillary electrophoresis of equilibrium mixtures: A universal tool for development of aptamers. J Am Chem Soc 127: 3165–3171.
18. Tok JB, Fischer NO (2008) Single microbead SELEX for efficient ssDNA aptamer generation against botulinum neurotoxin. Chem Comm. pp 1883–1885.
19. Jellinek D, Green LS, Bell C, Lynott CK, Gill N, et al. (1995) Potent 2′-amino-2′-deoxypyrimidine RNA inhibitors of basic fibroblast growth factor. Biochemistry 34: 11363–11372.
20. Pagratis NC, Bell C, Chang YF, Jennings S, Fitzwater T, et al. (1997) Potent 2′-amino-, and 2′-fluoro-2′-deoxyribonucleotide RNA inhibitors of keratinocyte growth factor. Nature Biotechnol 15: 68–73.
21. Chelliserrykattil J, Ellington AD (2004) Evolution of a T7 RNA polymerase variant that transcribes 2′-*O*-methyl RNA. Nature Biotechnol 22: 1155–1160.
22. Hernandez FJ, Kalra N, Wengel J, Vester B (2009) Aptamers as a model for functional evaluation of LNA and 2′-amino LNA. Bioorg Med Chem Lett 19: 6585–6587.
23. Schmidt KS, Borkowski S, Kurreck J, Stephens AW, Bald R, et al. (2004) Application of locked nucleic acids to improve aptamer in vivo stability and targeting function. Nucleic Acids Res 32: 5757–5765.
24. Kawasaki AM, Casper MD, Freier SM, Lesnik EA, Zounes MC, et al. (1993) Uniformly modified 2′-deoxy-2′-fluoro phosphorothioate oligonucleotides as nuclease-resistant antisense compounds with high affinity and specificity for RNA targets. J Med Chem 36: 831–841.
25. Somasunderam A, Ferguson MR, Rojo DR, Thiviyanathan V, Li X, et al. (2005) Combinatorial selection, inhibition, and antiviral activity of DNA thioaptamers targeting the RNase H domain of HIV-1 reverse transcriptase. Biochemistry 44: 10388–10395.
26. Boomer RM, Lewis SD, Healy JM, Kurz M, Wilson C, et al. (2005) Conjugation to polyethylene glycol polymer promotes aptamer biodistribution to healthy and inflamed tissues. Oligonucleotides 15: 183–195.
27. Kato T, Yano K, Ikebukuro K, Karube I (2000) Interaction of three-way DNA junctions with steroids. Nucleic Acids Res 28: 1963–1968.
28. Shangguan D, Tang Z, Mallikaratchy P, Xiao Z, Tan W (2007) Optimization and modifications of aptamers selected from live cancer cell lines. ChemBioChem 8: 603–606.
29. Sayer NM, Cubin M, Rhie A, Bullock M, Tahiri-Alaoui A, et al. (2004) Structural determinants of conformationally selective, prion-binding aptamers. J Biol Chem 279: 13102–13109.
30. Katilius E, Flores C, Woodbury NW (2007) Exploring the sequence space of a DNA aptamer using microarrays. Nucleic Acids Res 35: 7626–7635.
31. Houck KA, Ferrara N, Winer J, Cachianes G, Li B, et al. (1991) The vascular endothelial growth factor family: Identification of a fourth molecular species and characterization of alternative splicing of RNA. Mol Endocrinol 5: 1806–1814.
32. Park JE, Keller GA, Ferrara N (1993) The vascular endothelial growth factor (VEGF) isoforms: Differential deposition into the subepithelial extracellular matrix and bioactivity of extracellular matrix-bound VEGF. Mol Biol Cell 4: 1317–1326.
33. Cohen T, Gitay-Goren H, Sharon R, Shibuya M, Halaban R, et al. (1995) VEGF121, a vascular endothelial growth factor (VEGF) isoform lacking heparin binding ability, requires cell-surface heparan sulfates for efficient binding to the VEGF receptors of human melanoma cells. J Biol Chem 270: 11322–11326.
34. Keyt BA, Berleau LT, Nguyen HV, Chen H, Heinsohn H, et al. (1996) The carboxyl-terminal domain (111–165) of vascular endothelial growth factor is critical for its mitogenic potency. J Biol Chem 271: 7788–7795.
35. Hasegawa H, Sode K, Ikebukuro K (2008) Selection of DNA aptamers against VEGF165 using a protein competitor and the aptamer blotting method. Biotechnol Lett 30: 829–834.
36. Hasegawa H, Taira KI, Sode K, Ikebukuro K (2008) Improvement of aptamer affinity by dimerization. Sensors 8: 1090–1098.
37. Zuker M (2003) Mfold web server for nucleic acid folding and hybridization prediction. Nucleic Acids Res 31: 3406–3415.

38. Potty ASR, Kourentzi K, Fang H, Jackson GW, Zhang X, et al. (2009) Biophysical characterization of DNA aptamer interactions with vascular endothelial growth factor. Biopolymers 91: 145–156.
39. Davis KA, Lin Y, Abrams B, Jayasena SD (1998) Staining of cell surface human CD4 with 2′-F-pyrimidine-containing RNA aptamers for flow cytometry. Nucleic Acids Res 26: 3915–3924.
40. Daniels DA, Chen H, Hicke BJ, Swiderek KM, Gold L (2003) A tenascin-C aptamer identified by tumor cell SELEX: Systematic evolution of ligands by exponential enrichment. Proc Natl Acad Sci USA 100: 15416–15421.
41. Waleh NS, Brody MD, Knapp MA, Mendonca HL, Lord EM, et al. (1995) Mapping of the vascular endothelial growth factor-producing hypoxie cells in multicellular tumor spheroids using a hypoxia-specific marker. Cancer Res 55: 6222–6226.
42. Oswald J, Treite F, Haase C, Kampfrath T, Mäding P, et al. (2007) Experimental hypoxia is a potent stimulus for radiotracer uptake *in vitro*: Comparison of different tumor cells and primary endothelial cells. Cancer Lett 254: 102–110.
43. Calvani M, Trisciuoglio D, Bergamaschi C, Shoemaker RH, Melillo G (2008) Differential involvement of vascular endothelial growth factor in the survival of hypoxic colon cancer cells. Cancer Res 68: 285–291.
44. Vaupel P, Mayer A (2007) Hypoxia in cancer: Significance and impact on clinical outcome. Cancer Metast Rev 26: 225–239.
45. Minchenko A, Bauer T, Salceda S, Caro J (1994) Hypoxic stimulation of vascular endothelial growth factor expression in vitro and in vivo. Lab Invest 71: 374–379.
46. Neufeld G, Cohen T, Gengrinovitch S, Poltorak Z (1999) Vascular endothelial growth factor (VEGF) and its receptors. FASEB J 13: 9–22.
47. Ikeda E, Achen MG, Breier G, Risau W (1995) Hypoxia-induced transcriptional activation and increased mRNA stability of vascular endothelial growth factor in C6 glioma cells. J Biol Chem 270: 19761–19766.
48. Shima DT, Deutsch U, D'Amore PA (1995) Hypoxic induction of vascular endothelial growth factor (VEGF) in human epithelial cells is mediated by increases in mRNA stability. FEBS Lett 370: 203–208.